Dust semi-direct effects: Dust-induced longwave radiation influences low-level cloud response to free-tropospheric dust over the North Atlantic Ocean.

Satyendra K. Pandey and Adeyemi A. Adebiyi

Department of Life and Environmental Sciences, University of California - Merced, Merced, CA, USA

Supplementary Materials

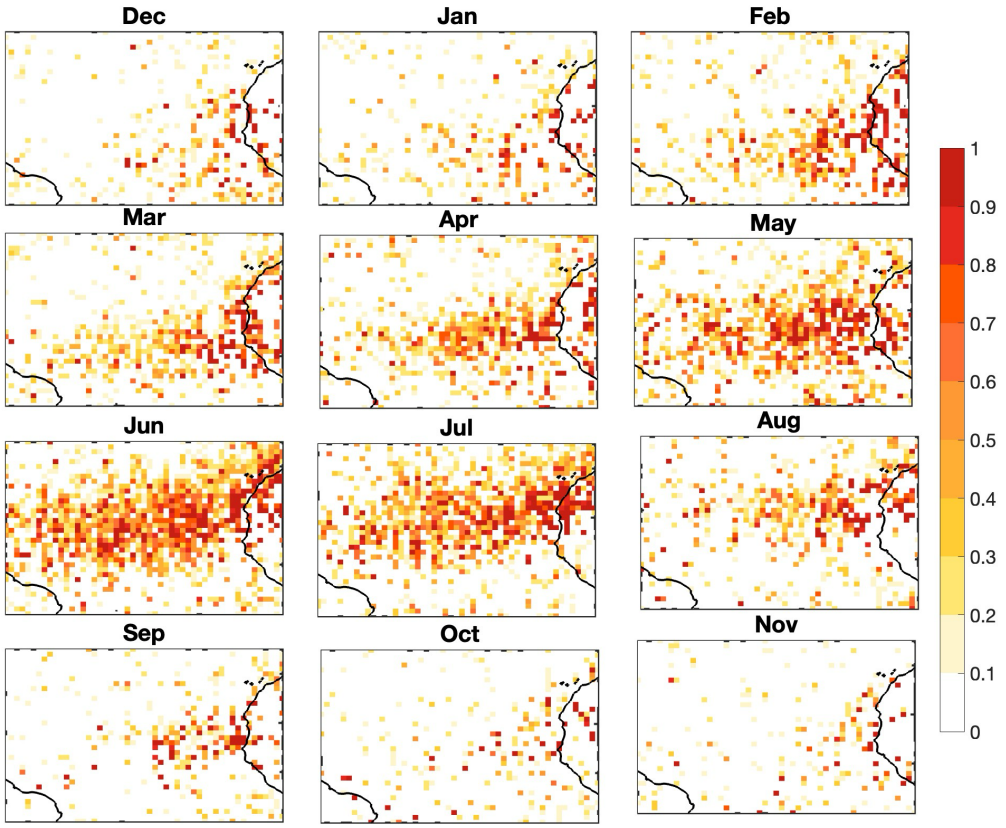

Figure S1: Probability of occurrence of dust above the low-level warm cloud using CALIPSO merged layer data.

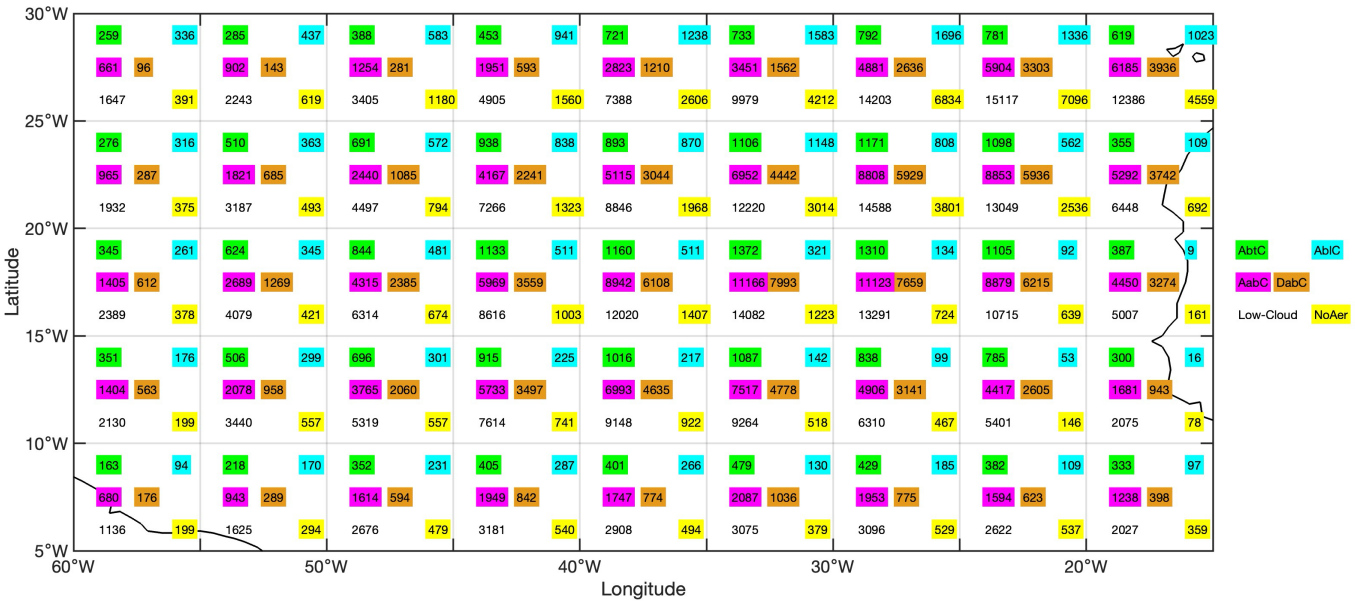

Figure S2: Number of samples in each 5˚×5˚ grid box, no shaded numbers show the total number of observed samples from 2007-2017, DabC (AabC) is dust (aerosol) above single-layer low-level clouds and shaded in golden (magenta) colors. Yellow shading is when only single-layer low-level clouds exist with no aerosol layer in the column. Cyan

(AblC) and green (AbtC) shaded numbers are profiles when aerosols are found below the cloud layer and aerosols on both sides of the cloud layers

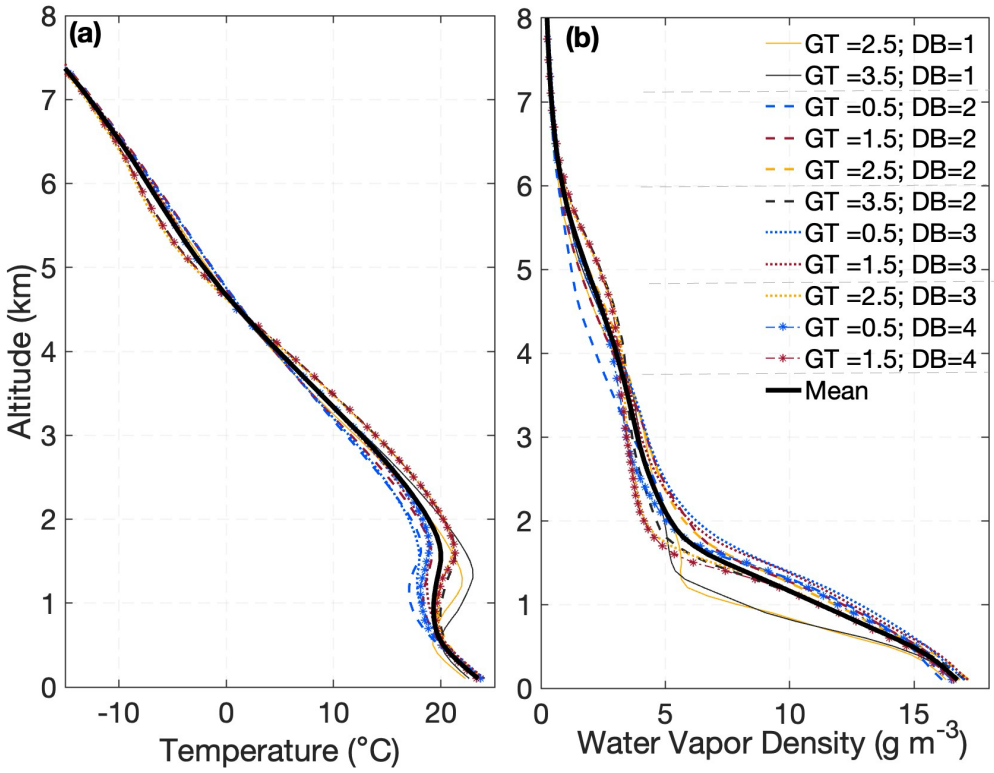

Figure S3: Profiles of (a) temperature and (b) humidity profiles used in SBDART to simulate radiative flux profiles correspond to the categories in Fig. 3. Thin lines in (a) and (b) are color-coded by geometric thickness (GT: blue = 0.5 km, red = 1.5 km, orange = 2.5 km, black = 3.5 km), while line styles represent base heights (DB: solid = 1 km, dashed = 2 km, dotted = 3 km, solid with markers = 4 km). The thick black line in panels (a) and (b) represents the mean values.

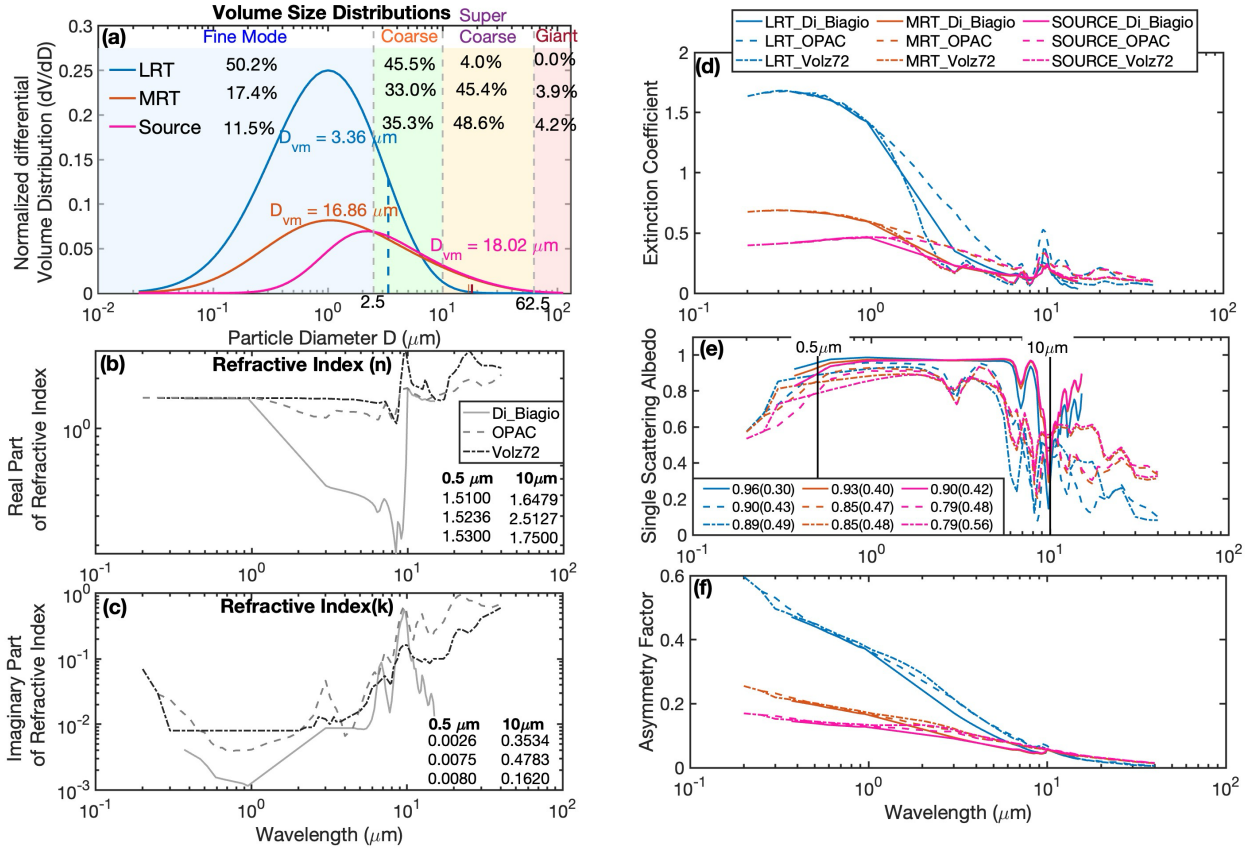

Figure S4: Input parameters used in SBDART to assess the impact of particle size and refractive index on dust-induced cloud-top heating. (a) particle size distribution, and spectral dependence of (b) real and (c) imaginary parts of the refractive index. Combinations of these size distributions and refractive indices were processed using Mie theory to compute the spectral variation of (d) extinction coefficient, (e) single scattering albedo (SSA), and (f) asymmetry parameters used as inputs for radiative transfer calculations. Three particle size categories represent dust near source regions (red lines), mid-range transport (orange lines), and long-range transport (blue lines), with volume mean diameters annotated in panel (a) with the same colors, 18.02 μm, 16.86 μm, and 3.36 μm, respectively. Refractive indices were taken from Di Biagio et al. (2019, solid lines), OPAC (Hess et al., 1998, dashed lines), and Volz (1972, dotted lines), capturing absorption variability due to aging and on panel (e), representative SSA at 0.5 μm (shortwave) and 10 μm (longwave), annotated as SSA_SW (SSA_LW), e.g., 0.99 (0.42), to illustrate spectral differences in absorption.

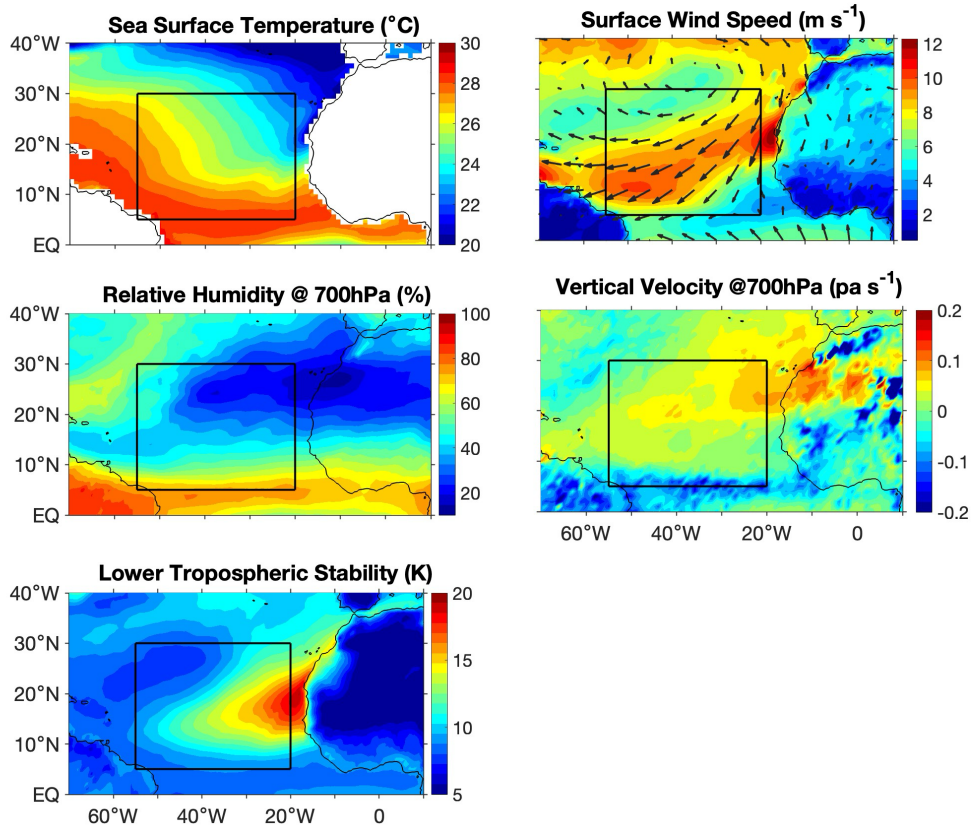

Figure S5: Climatological mean (from 2007 to 2017) of meteorological parameters relevant to the low-level cloud for the chosen months (May to August) over the selected domain. The black box shows the study region.

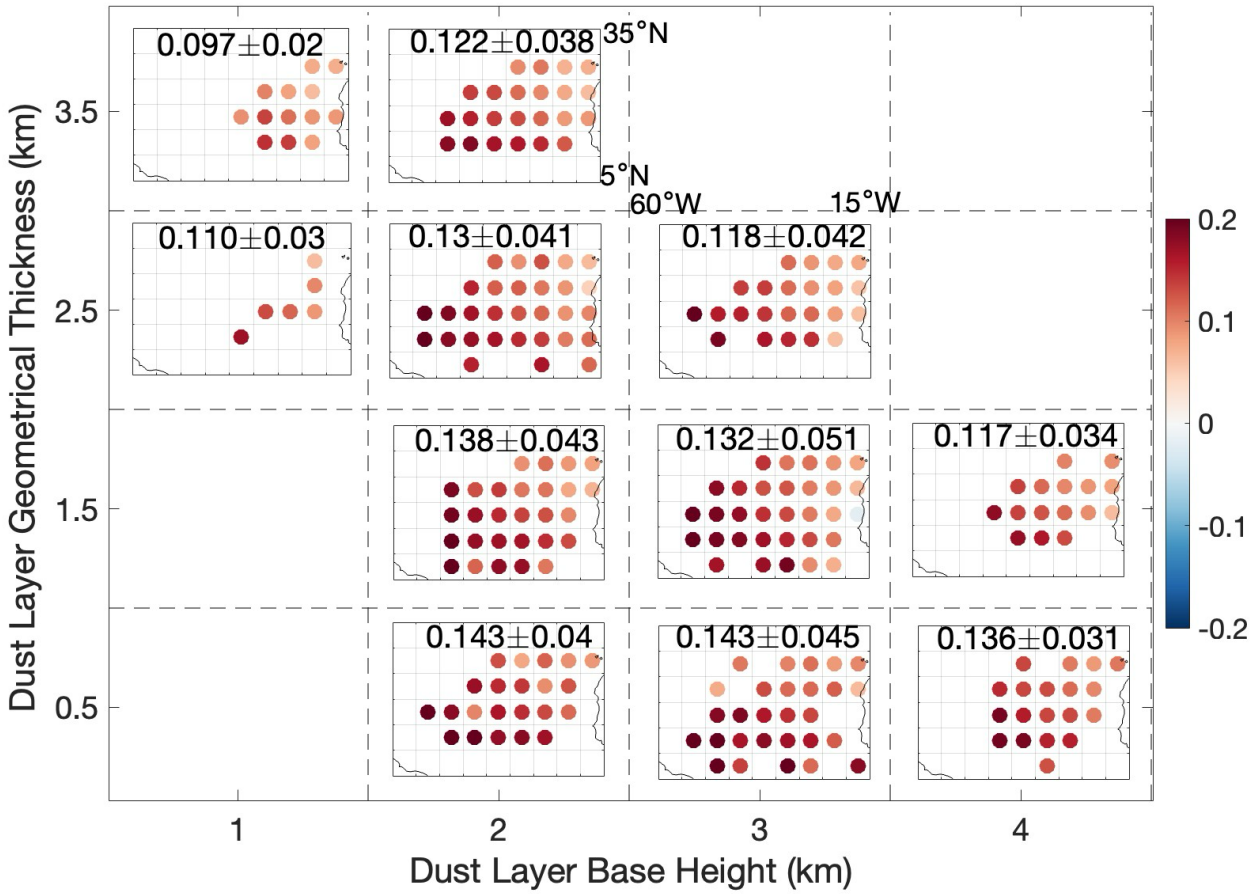

Figure S6: Location of grids used in averaging for each group in Fig 3. Colormap shows changes in cloud fraction anomalies. The average cloud fraction anomaly is shown for each category at the top of each subpanel.

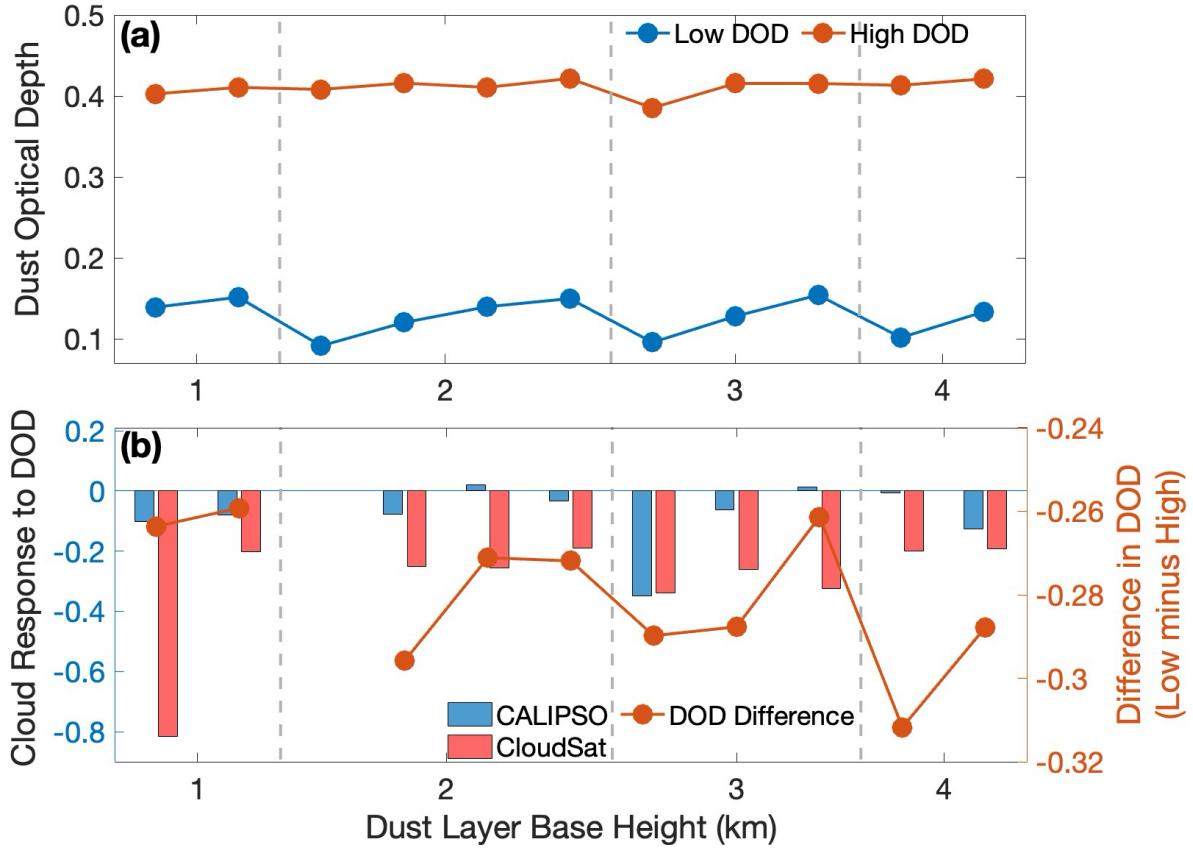

Figure S7: (a) Variation of low (blue line) and high (red line) dust optical depth across categories (b) Cloud response to dust optical depth ($\frac{\partial f'}{\partial DOD}$) shown corresponding to the left y-axis, blue bars using data from CALIPSO and red is from CloudSat, the difference in dust optical depth is shown by red line corresponding to right y-axis.

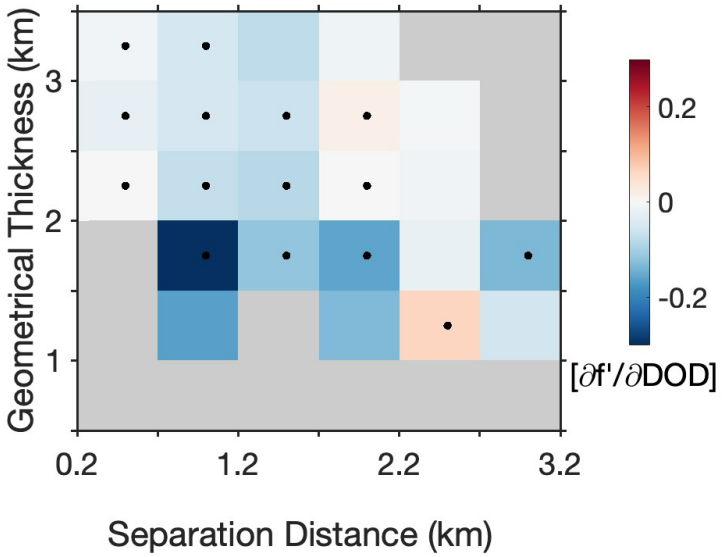

Figure S8: Change in *f'* per unit change in DOD as a function of dust base height and geometrical thickness

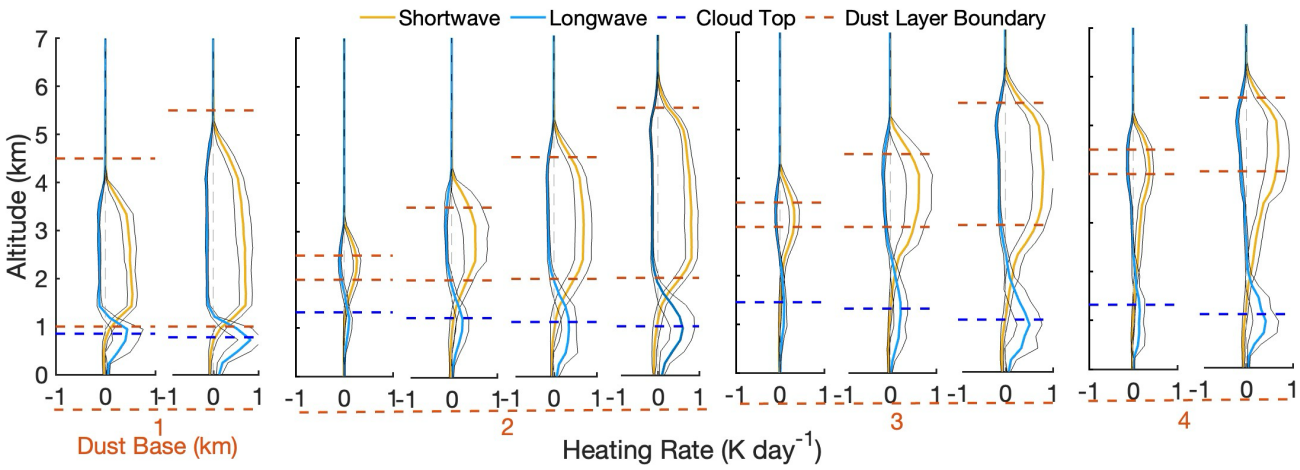

Figure S9: The dust-induced heating rate profiles for each category as shown in Fig 4. Yellow lines denote shortwave radiation, while cyan represents longwave radiation. The range around the lines represents the standard deviation. Similar to Fig 3, the profiles are grouped based on the dust base altitude, indicated by orange dashed lines at the bottom of the plots. Horizontal blue lines within the plot indicate the cloud top height, while orange colors mark the boundaries of the dust layer (base and top).

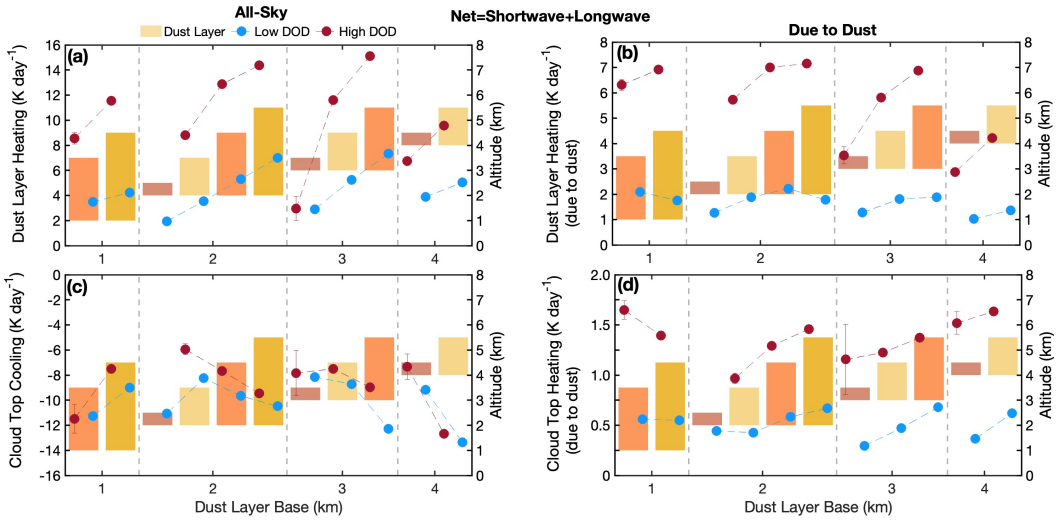

Figure S10: The Net (shortwave+longwave) heating rate (K day^{-1}) within the dust layer and at the cloud top categorized by dust layer base height and geometric thickness. The left panels show all-sky heating rates (a & c), and the right panels are due to dust (b&d). Bars represent the dust layer configurations shown in Figure 4. Blue circles indicate heating rates for low dust optical depth, while red circles indicate high dust optical depth. Error bars represent the standard error.

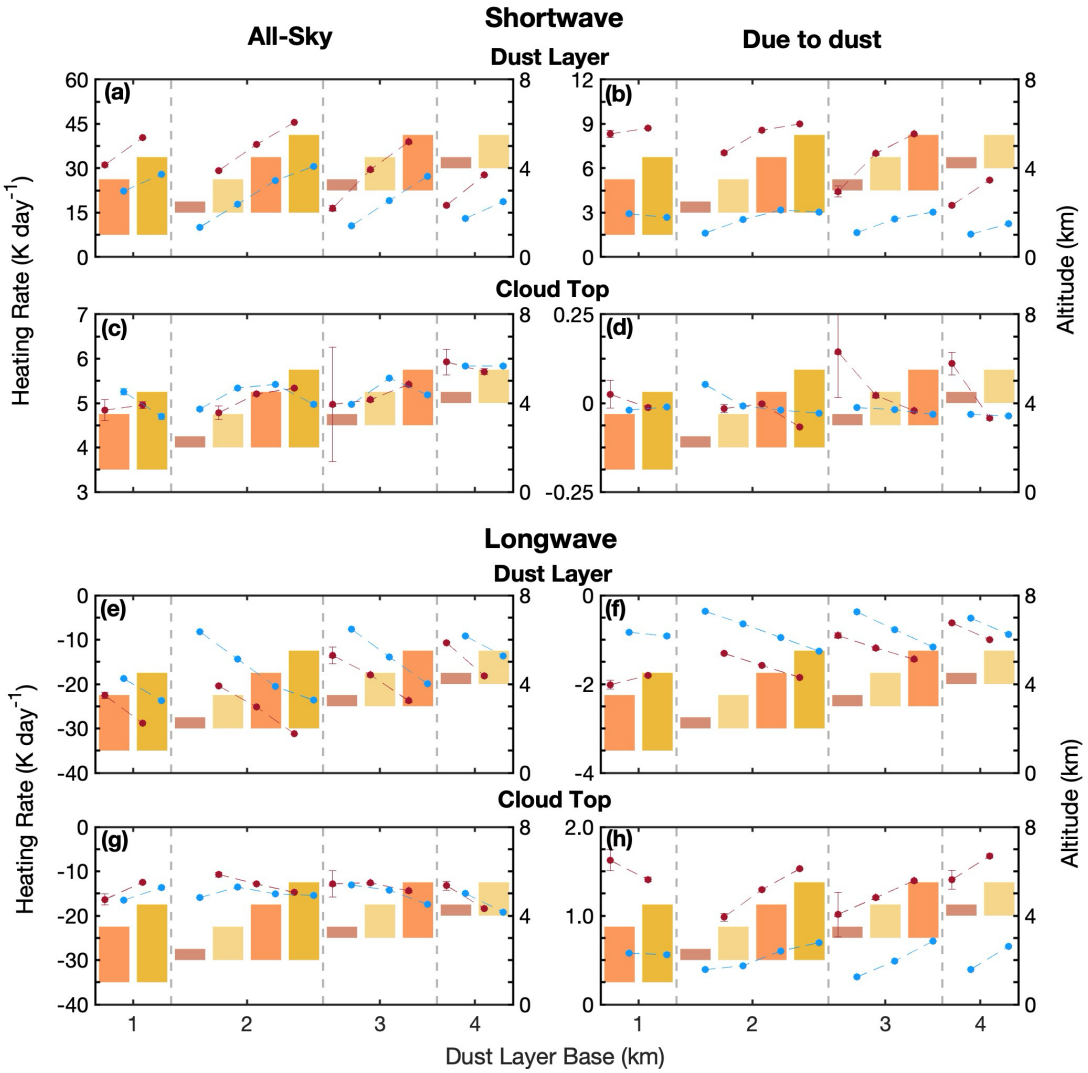

Figure S11: The shortwave (a, b,c & d) and longwave (e,f, g,h) part of the heating rate (K day^{-1}) within the dust layer and at the cloud top categorized by dust layer base height and geometric thickness. The left panels show all-sky heating rates (a,c,e & g), and the right panels are due to dust (b,d,f, &h). Bars represent the dust layer configurations shown in Figure 4. Blue circles indicate heating rates for low dust optical depth, while red circles indicate high dust optical depth. Error bars represent the standard error.

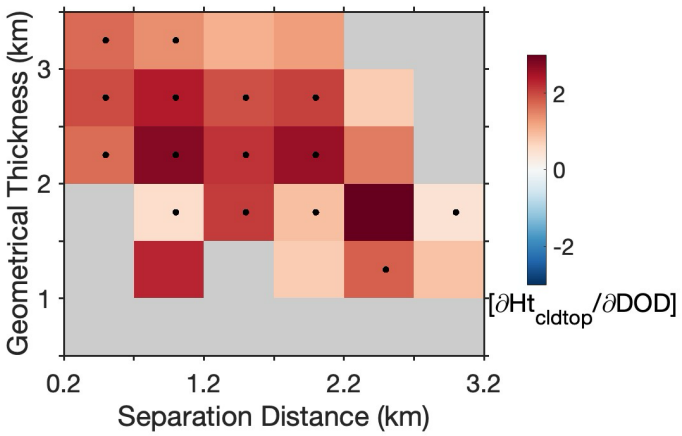

Figure S12: Change in dust-induced cloud top heating per unit change in DOD$\left(\frac{\partial Ht_{cldtop}}{\partial DOD}\ (K\ day^{-1}\ DOD^{-1})\right)$ as a function of dust base height and geometrical thickness

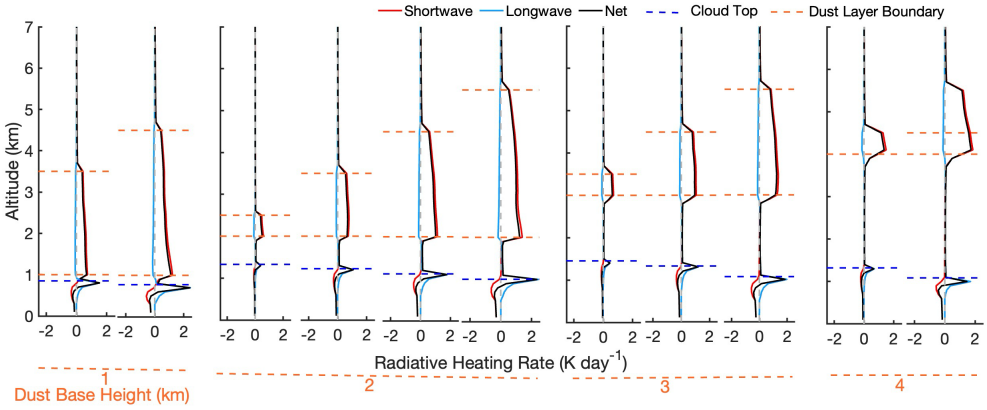

Figure S13: SBDART-simulated vertical profiles of radiative heating rates due to dust, based on the size distribution categories defined in Fig. 3 (compare it with Fig. S9). The simulations used a long-range transported dust particle size distribution (blue line in Fig S4a) and Di Biagio et al. (2019) refractive index (solid grey-line in Fig S4b&c). Red lines indicate shortwave (SW) heating, blue lines represent longwave (LW) heating, and black lines show the net radiative effect. The blue dotted horizontal line marks the cloud top, and the orange lines denote the vertical boundaries of the dust layer.

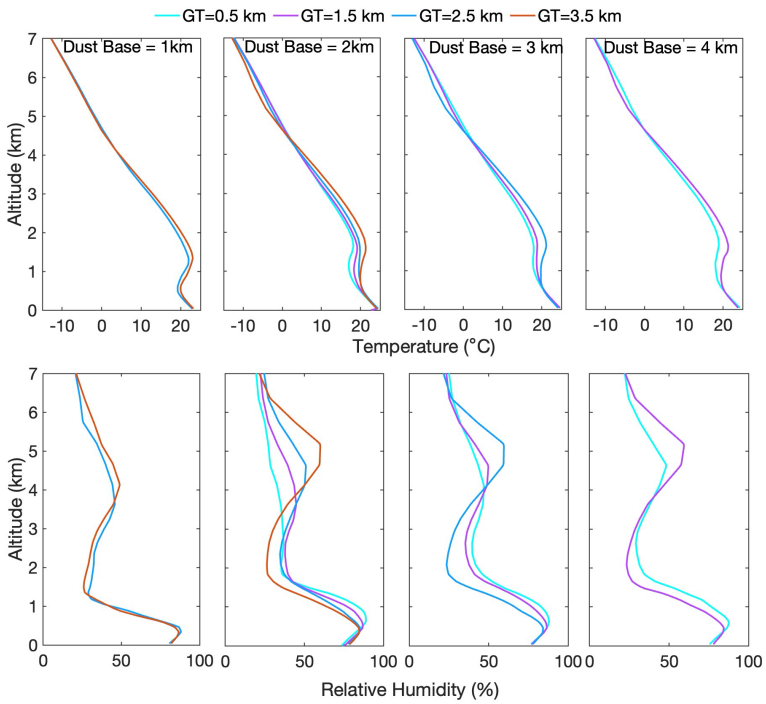

Figure S14: Temperature (upper panels) and relative humidity (lower panels) profiles corresponding to 11 categories grouped based on dust base height. Profiles corresponding to equal dust-layer geometrical thickness are shown by the same colors, with cyan color for a geometric thickness of 0.5km, magenta for 1.5km, blue for 2.5 km, and orange for 3.5km.

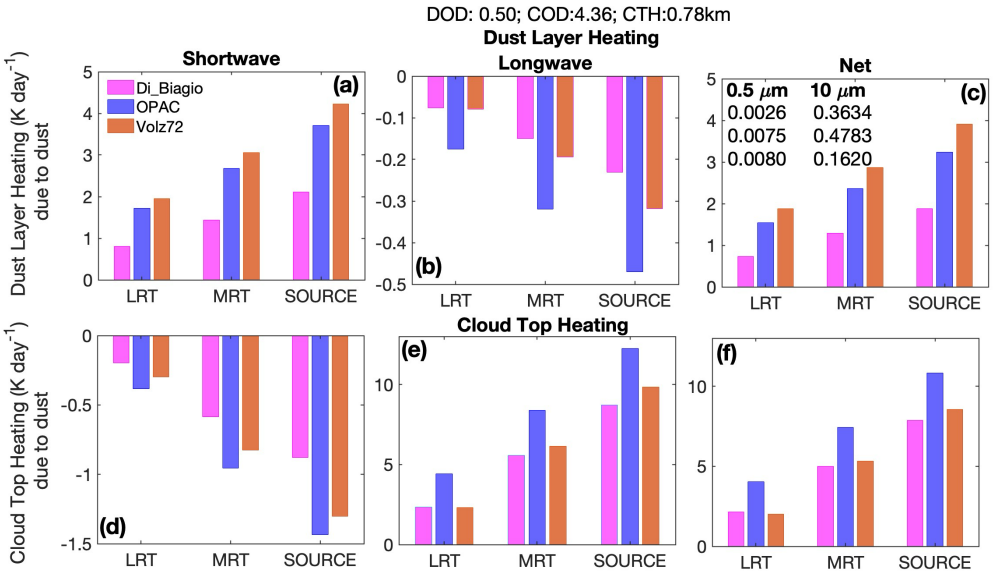

Figure S15: SBDART-simulated dust-induced heating within the dust layer (a–c) and at the cloud top (d–f), for fixed thermodynamic profile, dust optical depth (0.50), cloud optical depth (4.36), cloud top height (0.78 km), dust layer base height (2km) and geometric thickness (2.5km). Panels show shortwave (a, d), longwave (b, e), and net heating (c, f). The x-axis represents particle size distributions corresponding to long-range transport (LRT), medium-range transport (MRT), and source regions. Bar colors indicate refractive index: magenta for Di Biagio, blue for OPAC, and orange for Volz72. Numbers in panel (c) denote the imaginary part of the refractive index at 0.5 μm and 10 μm.

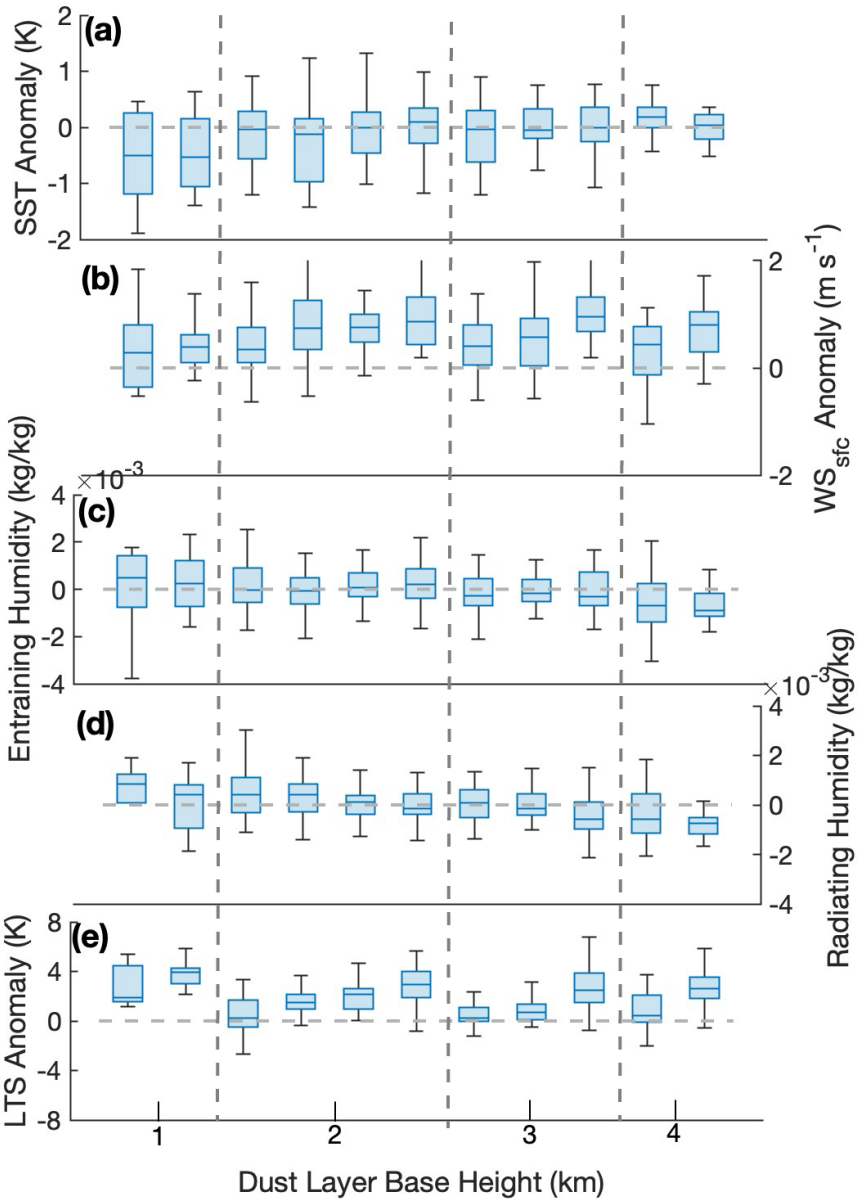

Figure S16: Box and whisker plot showing variation in (a) sea surface temperature, (b) surface wind speed, (c) entraining and (d) radiating humidity, and (e) lower tropospheric stability across the categories.

Table S1: Dust layer and cloud parameters used in the model simulations for control and sensitivity experiments, designed to isolate the effects of dust properties from the background thermodynamic profile and cloud properties on dust-induced cloud-top heating sensitivities to geometrical thickness $\frac{\partial CldTpHt_{dust}}{\partial GT}\Big|_{DB}$ and dust base height $\frac{\partial CldTpHt_{dust}}{\partial DB}\Big|_{GT}$, under fixed dust base (DB) and geometrical thickness (GT), respectively. Bold fonts indicate parameters that vary across categories; all others remain fixed. vSt1, vSt2, etc., refer to the vertical structure per category. Th1, Th2, Th3, etc., represent thermodynamic profiles for categories 1, 2, 3, and so on. DOD1, DOD2, DOD3, etc., denote dust optical depths, and COD1, COD2, COD3, etc., indicate cloud optical depths. Note: In Experiments 1 and 3, variation in cloud boundaries across categories is allowed, while Experiments 2 and 4 use fixed cloud boundaries corresponding to Category 2, with a cloud top height of 0.78 km and a cloud base height of 0.43 km.

(Exp-1)	**Control Simulation (Variation in all parameters allowed across category)**											
	Cat1	**Cat2**	**Cat3**	**Cat4**	**Cat5**	**Cat6**	**Cat7**	**Cat 8**	**Cat9**	**Cat10**	**Cat11**	**Mean**
Dust Layer Base Height (km)	**1**	**1**	**2**	**2**	**2**	**2**	**3**	**3**	**3**	**4**	**4**	
Geometric Thickness (km)	**2.5** vSt1	**3.5** vSt2	**0.5** vSt3	**1.5** vSt4	**2.5** vSt5	**3.5** vSt6	**0.5** vSt7	**1.5** vSt8	**2.5** vSt9	**0.5** vSt10	**1.5** vSt11	
Thermodynamic Profile	**Th1**	**Th2**	**Th3**	**Th4**	**Th5**	**Th6**	**Th7**	**Th8**	**Th9**	**Th10**	**Th11**	
Dust Optical Depth	**0.23** DOD1	**0.42** DOD2	**0.05** DOD3	**0.18** DOD4	**0.35** DOD5	**0.50** DOD6	**0.08** DOD6	**0.24** DOD8	**0.41** DOD9	**0.12** DOD10	**0.30** DOD11	**0.26**
Cloud Optical Depth	**6.05** COD1	**4.54** COD2	**6.95** COD3	**6.39** COD4	**4.76** COD5	**4.36** COD6	**6.36** COD7	**5.52** COD8	**4.82** COD9	**6.70** COD10	**6.30** COD11	**5.70**
Cloud Top Height (km)	**0.85**	**0.78**	**1.33**	**1.22**	**1.12**	**1.00**	**1.45**	**1.32**	**1.06**	**1.32**	**1.09**	**1.14**
Cloud Base Height (km)	**0.46**	**0.43**	**0.84**	**0.79**	**0.71**	**0.64**	**0.94**	**0.86**	**0.70**	**0.86**	**0.71**	**0.72**
(Exp-2)	**Dust Properties (Dust-Categories and DOD variation allowed)**											Number of Simulations 11Th×11COD=121
Dust Layer Base Height (km)	**1**	**1**	**2**	**2**	**2**	**2**	**3**	**3**	**3**	**4**	**4**	
Geometric Thickness (km)	**2.5**	**3.5**	**0.5**	**1.5**	**2.5**	**3.5**	**0.5**	**1.5**	**2.5**	**0.5**	**1.5**	
Thermodynamic Profile	Th1	Th1	Th1	Th1	Th1	Th1	Th1	Th1	Th1	Th1	Th1	Th1,Th2…Th11
Dust Optical Depth	**0.23**	**0.42**	**0.05**	**0.18**	**0.35**	**0.50**	**0.08**	**0.24**	**0.41**	**0.12**	**0.30**	
Cloud Optical Depth	6.05	6.05	6.05	6.05	6.05	6.05	6.05	6.05	6.05	6.05	6.05	COD1, COD2…COD11
Cloud Top Height (km)	0.78	0.78	0.78	0.78	0.78	0.78	0.78	0.78	0.78	0.78	0.78	
Cloud Base Height (km)	0.43	0.43	0.43	0.43	0.43	0.43	0.43	0.43	0.43	0.43	0.43	
(Exp-3)	**Cloud Properties (COD and Cloud Boundaries varry)**											Number of Simulations 11vSt×11Th×11DOD=1331
Dust Layer Base Height (km)	1	1	1	1	1	1	1	1	1	1	1	vSt1,vStt2,..vSt11
Geometric Thickness (km)	2.5	2.5	2.5	2.5	2.5	2.5	2.5	2.5	2.5	2.5	2.5	
Thermodynamic Profile	Th1	Th1	Th1	Th1	Th1	Th1	Th1	Th1	Th1	Th1	Th1	Th1,Th2,...Th11
Dust Optical Depth	0.23	0.23	0.23	0.23	0.23	0.23	0.23	0.23	0.23	0.23	0.23	DOD1,DOD2...DOD11
Cloud Optical Depth	**6.05**	**4.54**	**6.95**	**6.39**	**4.76**	**4.36**	**6.36**	**5.52**	**4.82**	**6.70**	**6.30**	
Cloud Top Height (km)	**0.85**	**0.78**	**1.33**	**1.22**	**1.12**	**1.00**	**1.45**	**1.32**	**1.06**	**1.32**	**1.09**	
Cloud Base Height (km)	**0.46**	**0.43**	**0.84**	**0.79**	**0.71**	**0.64**	**0.94**	**0.86**	**0.70**	**0.86**	**0.71**	
(Exp-4)	**Thermodynamic Profile**											Number of Simulations 11vSt×11DOD×11COD=1331
Dust Layer Base Height (km)	1	1	1	1	1	1	1	1	1	1	1	vSt1,vSt2…vSt11
Geometric Thickness (km)	2.5	2.5	2.5	2.5	2.5	2.5	2.5	2.5	2.5	2.5	2.5	
Thermodynamic Profile	**Th1**	**Th2**	**Th3**	**Th4**	**Th5**	**Th6**	**Th7**	**Th8**	**Th9**	**Th10**	**Th11**	
Dust Optical Depth	0.23	0.23	0.23	0.23	0.23	0.23	0.23	0.23	0.23	0.23	0.23	DOD1,DOD2,..DOD11
Cloud Optical Depth	6.05	6.05	6.05	6.05	6.05	6.05	6.05	6.05	6.05	6.05	6.05	COD1,COD2,...COD11
Cloud Top Height (km)	0.78	0.78	0.78	0.78	0.78	0.78	0.78	0.78	0.78	0.78	0.78	
Cloud Base Height (km)	0.43	0.43	0.43	0.43	0.43	0.43	0.43	0.43	0.43	0.43	0.43	